Supplementary Material:
Optimizing imaging speed and excitation intensity for single molecule localization microscopy

Robin Diekmann[a], Maurice Kahnwald[a,b], Andreas Schoenit[a], Joran Deschamps[a], Ulf Matti[a], Jonas Ries[a,*]

[a] *EMBL, Cell Biology and Biophysics, Heidelberg, Germany*

[b] *Current affiliation: Friedrich Miescher Institute for Biomedical Research, Basel, Switzerland*

Index

Supplementary Table 1: Results of image analysis.

Sample / buffer	Intensity (kW/cm^2) / camera exposure time (ms) / effective laser exposure time (ms)	Effective labeling efficiency (%)	Photons per localization	Localizations per NPC	Localizations per fluorophore	N / cells / NPCs analyzed
Nup96-SNAP-BG-AF647	0.36/500/498.45	65 ± 12	20917 ± 4746	246 ± 109	11.5 ± 3.9	3 / 4 / 1123
	0.73/250/248.45	63 ± 2	21960 ± 3026	119 ± 25	6.0 ± 1.2	1 / 6 / 1282
	1.6/116/114.45	62 ± 2	13159 ± 597	106 ± 25	5.3 ± 1.1	2 / 5 / 1307
GLOX+BME	3.2/59/57.45	64 ± 4	11917 ± 740	111 ± 23	5.5 ± 1.0	3 / 6 / 1883
	6.4/30/28.45	60 ± 4	10364 ± 366	83 ± 13	4.3 ± 0.5	6 / 10 / 3972
	13/16/14.45	56 ± 2	8890 ± 429	61 ± 6	3.5 ± 0.4	2 / 6 / 1757
	24/9/7.45	48 ± 2	7645 ± 240	42 ± 3	2.7 ± 0.2	2 / 7 / 2130
	53/5/3.45	40 ± 3	5889 ± 143	25 ± 1	2.0 ± 0.1	2 / 6 / 1739
	74/4/2.45	39 ± 3	5014 ± 266	22 ± 2	1.8 ± 0.1	2 / 6 / 1719
	120/3/1.45	30 ± 2	3896 ± 144	15 ± 1	1.5 ± 0.1	2 / 6 / 1411
	250/3/0.725	25 ± 2	2735 ± 126	10 ± 1	1.3 ± 0.0	2 / 6 / 818
	480/3/0.375	22 ± 2	1895 ± 60	8 ± 1	1.2 ± 0.1	2 / 6 / 345
Nup96-SNAP-BG-AF647	0.36/500/498.45	60 ± 4	11174 ± 675	99 ± 17	5.1 ± 0.8	3 / 3 / 897
	1.6/116/114.45	54 ± 2	10354 ± 2414	76 ± 14	4.4 ± 0.8	4 / 9 / 3060
	3.2/59/57.45	56 ± 2	8302 ± 297	78 ± 12	4.4 ± 0.6	3 / 6 / 1814
GLOX+MEA	6.4/30/28.45	53 ± 3	7755 ± 1040	62 ± 17	3.7 ± 0.9	5 / 10 / 3451
	13/16/14.45	54 ± 3	6969 ± 970	59 ± 10	3.4 ± 0.4	3 / 6 / 2167
	24/9/7.45	50 ± 3	6056 ± 837	43 ± 5	2.7 ± 0.2	3 / 6 / 2100
	53/5/3.45	44 ± 2	4992 ± 277	30 ± 1	2.1 ± 0.1	2 / 6 / 1782
	74/4/2.45	41 ± 2	4592 ± 203	24 ± 1	1.8 ± 0.1	2 / 8 / 2146
	120/3/1.45	37 ± 1	3380 ± 123	18 ± 1	1.6 ± 0.0	2 / 9 / 2427
	250/3/0.725	32 ± 1	2655 ± 123	13 ± 1	1.3 ± 0.1	2 / 8 / 1653
	480/3/0.375	29 ± 3	2027 ± 95	11 ± 1	1.2 ± 0.0	2 / 6 / 973
Nup96-SNAP-BG-AF647	0.36/500/498.45	68 ± 6	24901 ± 1403	216 ± 77	9.7 ± 2.6	3 / 3 / 1721
	1.6/116/114.45	64 ± 2	16676 ± 532	102 ± 28	4.9 ± 1.2	3 / 5 / 2781
	6.4/30/28.45	60 ± 6	11194 ± 955	59 ± 11	3.0 ± 0.4	3 / 5 / 3267
GLOX+BME	24/9/7.45	53 ± 5	5984 ± 377	40 ± 14	2.4 ± 1.1	2 / 5 / 2624
refractive index	53/5/3.45	49 ± 7	3838 ± 483	27 ± 4	1.7 ± 0.0	2 / 5 / 2584
matched	120/3/1.45	36 ± 6	2600 ± 352	16 ± 3	1.4 ± 0.1	2 / 6 / 2780
(n = 1.4)	250/3/0.725	26 ± 7	1951 ± 61	10 ± 3	1.3 ± 0.0	2 / 5 / 1371
Nup96-mEGFP-AB-AF647	0.36/500/498.45	67 ± 5	15654 ± 1698	210 ± 10	n.a.	2 / 4 / 1026
	1.6/116/114.45	69 ± 3	12473 ± 833	251 ± 54	n.a.	2 / 6 / 1494
	6.4/30/28.45	70 ± 3	9935 ± 637	176 ± 25	n.a.	2 / 6 / 1716
GLOX+BME	24/9/7.45	60 ± 2	7666 ± 429	104 ± 13	n.a.	2 / 6 / 1668
	53/5/3.45	53 ± 6	6301 ± 320	79 ± 19	n.a.	2 / 6 / 1711
	120/3/1.45	46 ± 4	4538 ± 170	46 ± 7	n.a.	2 / 6 / 1617
	250/3/0.725	33 ± 3	2386 ± 71	20 ± 4	n.a.	2 / 6 / 1513
Nup96-mEGFP-NB-CF680	6.4/30/28.45	53 ± 5	6206 ± 394	144 ± 19	n.a.	3 / 10 / 2458
	24/9/7.45	42 ± 5	5149 ± 340	79 ± 5	n.a.	3 / 8 / 1616
	53/5/3.45	37 ± 4	4658 ± 174	61 ± 5	n.a.	2 / 6 / 1449
GLOX+BME	120/3/1.45	34 ± 4	4074 ± 168	46 ± 8	n.a.	2 / 5 / 1004
	250/3/0.725	24 ± 2	3632 ± 951	20 ± 2	n.a.	2 / 6 / 827
Nup96-mEGFP-AB-CF660C	6.4/30/28.45	70 ± 3	15850 ± 2474	189 ± 16	n.a.	2 / 8 / 2176
	24/9/7.45	73 ± 5	9581 ± 1408	202 ± 26	n.a.	2 / 8 / 1988
	53/5/3.45	69 ± 7	7051 ± 1454	171 ± 54	n.a.	2 / 5 / 1145
GLOX+BME	120/3/1.45	68 ± 8	5151 ± 821	139 ± 28	n.a.	2 / 8 / 1785
	250/3/0.725	55 ± 7	3045 ± 356	68 ± 12	n.a.	2 / 8 / 1930
Nup96-mEGFP-AB-Dy634	0.36/500/498.45	51 ± 4	8905 ± 946	241 ± 54	n.a.	3 / 4 / 1095
	1.6/116/114.45	52 ± 9	5392 ± 599	246 ± 103	n.a.	3 / 6 / 2239

	6.4/30/28.45	52 ± 3	3768 ± 302	157 ± 29	n.a.	2 / 5 / 1551
GLOX+BME	24/9/7.45	42 ± 5	3529 ± 213	80 ± 15	n.a.	2 / 6 / 1867
	53/5/3.45	42 ± 8	3208 ± 191	88 ± 52	n.a.	2 / 10 / 4061
	120/3/1.45	40 ± 6	3044 ± 155	60 ± 13	n.a.	2 / 6 / 2115
	250/3/0.725	39 ± 8	2660 ± 195	56 ± 24	n.a.	3 / 6 / 1813
Microtubule-AB-AF647	0.36/500/498.45	n.a.	21869 ± 5244	n.a.	n.a.	2 / 3 / n.a.
	1.6/116/114.45	n.a.	11561 ± 1569	n.a.	n.a.	2 / 5 / n.a.
	6.4/30/28.45	n.a.	11597 ± 2918	n.a.	n.a.	2 / 5 / n.a.
GLOX+BME	24/9/7.45	n.a.	8320 ± 887	n.a.	n.a.	2 / 6 / n.a.
	53/5/3.45	n.a.	6377 ± 750	n.a.	n.a.	2 / 6 / n.a.
	120/3/1.45	n.a.	4202 ± 324	n.a.	n.a.	2 / 7 / n.a.
	250/3/0.725	n.a.	2256 ± 101	n.a.	n.a.	2 / 7 / n.a.
Nup96-mMaple	0.48/195/193.45	52 ± 5	1922 ± 132	68 ± 14	4.0 ± 0.5	2 / 6 / 2318
	0.94/99/97.45	53 ± 7	1825 ± 133	72 ± 19	4.2 ± 0.7	3 / 6 / 2664
Tris in D_2O	1.9/50/48.45	55 ± 3	1815 ± 102	80 ± 7	4.6 ± 0.3	3 / 8 / 3652
	3.8/26/24.45	52 ± 6	1691 ± 105	66 ± 13	4.0 ± 0.4	3 / 7 / 3369
	7.5/14/12.45	50 ± 4	1498 ± 80	59 ± 11	3.6 ± 0.4	2 / 6 / 2912
	14/8/6.45	50 ± 4	1230 ± 78	53 ± 4	3.3 ± 0.1	2 / 7 / 3764
	27/5/3.45	44 ± 3	905 ± 34	39 ± 4	2.7 ± 0.2	2 / 6 / 2765
	38/4/2.45	39 ± 3	684 ± 46	29 ± 3	2.3 ± 0.1	2 / 7 / 1858
	64/3/1.45	34 ± 3	509 ± 23	22 ± 1	2.0 ± 0.1	2 / 6 / 1779
	130/3/0.725	22 ± 3	314 ± 6	11 ± 2	1.5 ± 0.1	2 / 6 / 1069
Nup96-SNAP-BG-AF647	0.36/50*/49.85*	55 ± 3	4709 ± 255	32 ± 3	1.8 ± 0.1	2 / 9 / 2987
	1.6/11.6*/11.45*	52 ± 1	4588 ± 300	31 ± 2	1.8 ± 0.1	2 / 9 / 2617
Offswitching experiment	6.4/3*/2.85*	50 ± 2	4524 ± 203	29 ± 2	1.8 ± 0.1	2 / 9 / 2992
	24/0.9*/0.75*	42 ± 3	4613 ± 358	24 ± 2	1.8 ± 0.1	2 / 9 / 2949
	53/0.5*/0.35*	38 ± 7	4850 ± 451	22 ± 5	1.8 ± 0.1	2 / 9 / 2672
GLOX+BME	120/0.3*/0.15*	30 ± 3	4488 ± 244	18 ± 2	1.9 ± 0.0	2 / 9 / 2598
Imaging at 1.25 ms eff. laser exp. and 61 kW/cm^2 intensity	480/0.3*/0.038*	28 ± 3	4824 ± 350	16 ± 2	1.8 ± 0.1	2 / 9 / 2352
Nup96-SNAP-BG-AF647	0.36/50s*/49.85s*	57 ± 2	7723 ± 772	44 ± 5	2.4 ± 0.3	2 / 7 / 2021
	1.6/11.6s*/11.45s*	54 ± 2	7752 ± 337	42 ± 2	2.4 ± 0.1	2 / 7 / 1799
Offswitching experiment	6.4/3s*/2.85s*	50 ± 2	7726 ± 590	39 ± 3	2.4 ± 0.2	2 / 7 / 1855
	24/0.9s*/0.75s*	43 ± 3	7736 ± 655	34 ± 3	2.5 ± 0.1	2 / 9 / 2437
	53/0.5s*/0.35s*	38 ± 2	8240 ± 358	30 ± 2	2.5 ± 0.1	2 / 7 / 1719
GLOX+BME	120/0.3s*/0.15s*	35 ± 3	7829 ± 448	29 ± 3	2.6 ± 0.1	2 / 7 / 1857
Imaging at 7.5 ms eff. laser exp. and 24 kW/cm^2 intensity	480/0.3s*/0.038s*	31 ± 2	8039 ± 272	25 ± 2	2.5 ± 0.1	2 / 7 / 1870

*Values correspond to intensity and exposure time during initial off-switching phase

Results of image analysis.

Values show mean ± standard deviation. N depicts the number of biologically independent experiments. See Supplementary Dataset 1 for all individual data points.

Supplementary Figure 1: Off-switching

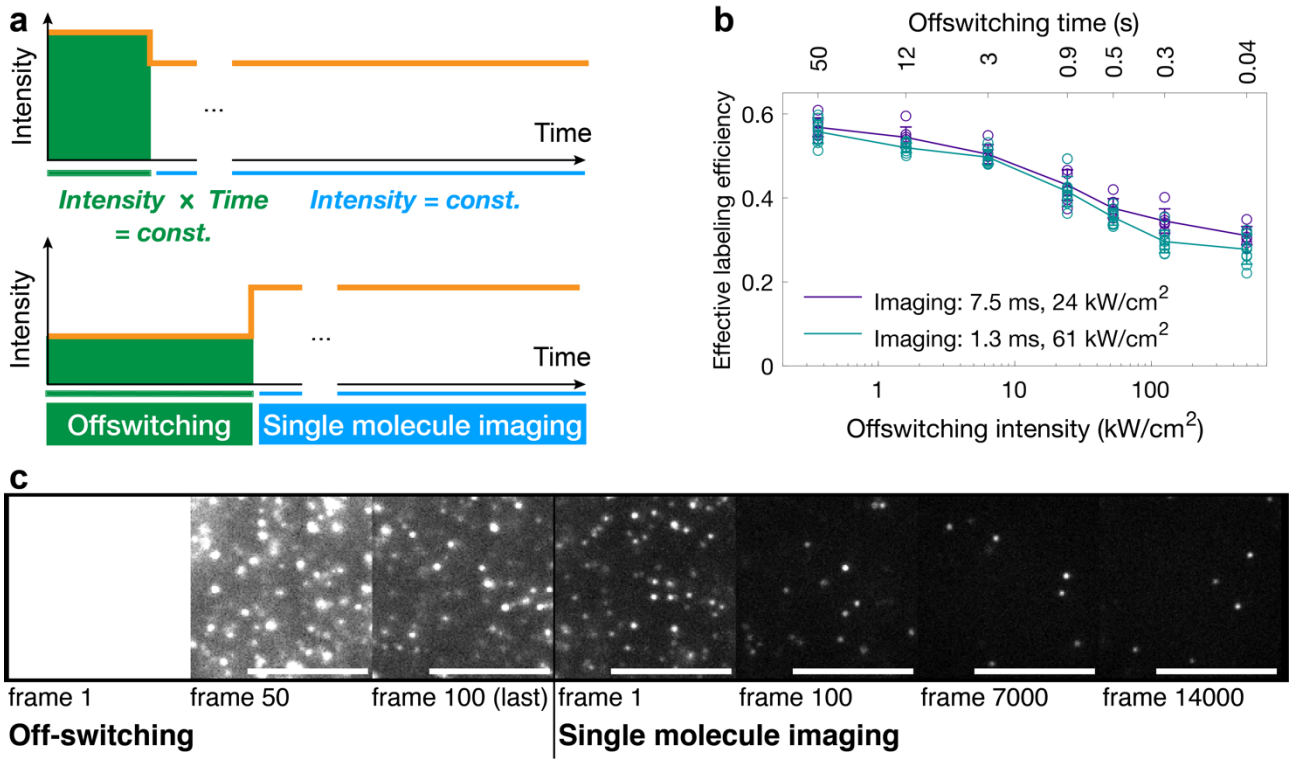

Off-switching

a, Experimental design to evaluate the influence of different intensities during the off-switching phase on the effective labeling efficiency. The time of the off-switching phase is adjusted to the intensities (ranging from 0.36 kW/cm^2 to 480 kW/cm^2) such that the light dose, i.e. the product of time and intensity, is constant for all conditions. A different, but constant intensity is applied during the subsequent single molecule imaging phase, from which the SMLM data is reconstructed and the labeling efficiency is determined. **b**, Effective labeling efficiency as a function of the different off-switching intensities, recorded at identical imaging intensities. See Supplementary Table 1 for sample size and replicates. **c**, Representative raw data of the off-switching phase (intensity of 6.4 kW/cm^2) and the subsequent single molecule imaging phase (intensity of 61 kW/cm^2). During the off-switching phase, individual emitters are not clearly separated such that single molecule localization is not possible. Scalebar, 10 µm. See Supplementary Table 1 for an overview about sample size and replicates and Supplementary Dataset 1 for detailed information about each measurement. All images scaled 0 - 303 photons/pixel/frame. Error bars denote mean ± standard deviation.

Supplementary Figure 2: Nup96-SNAP-AF647 in 143 mM BME

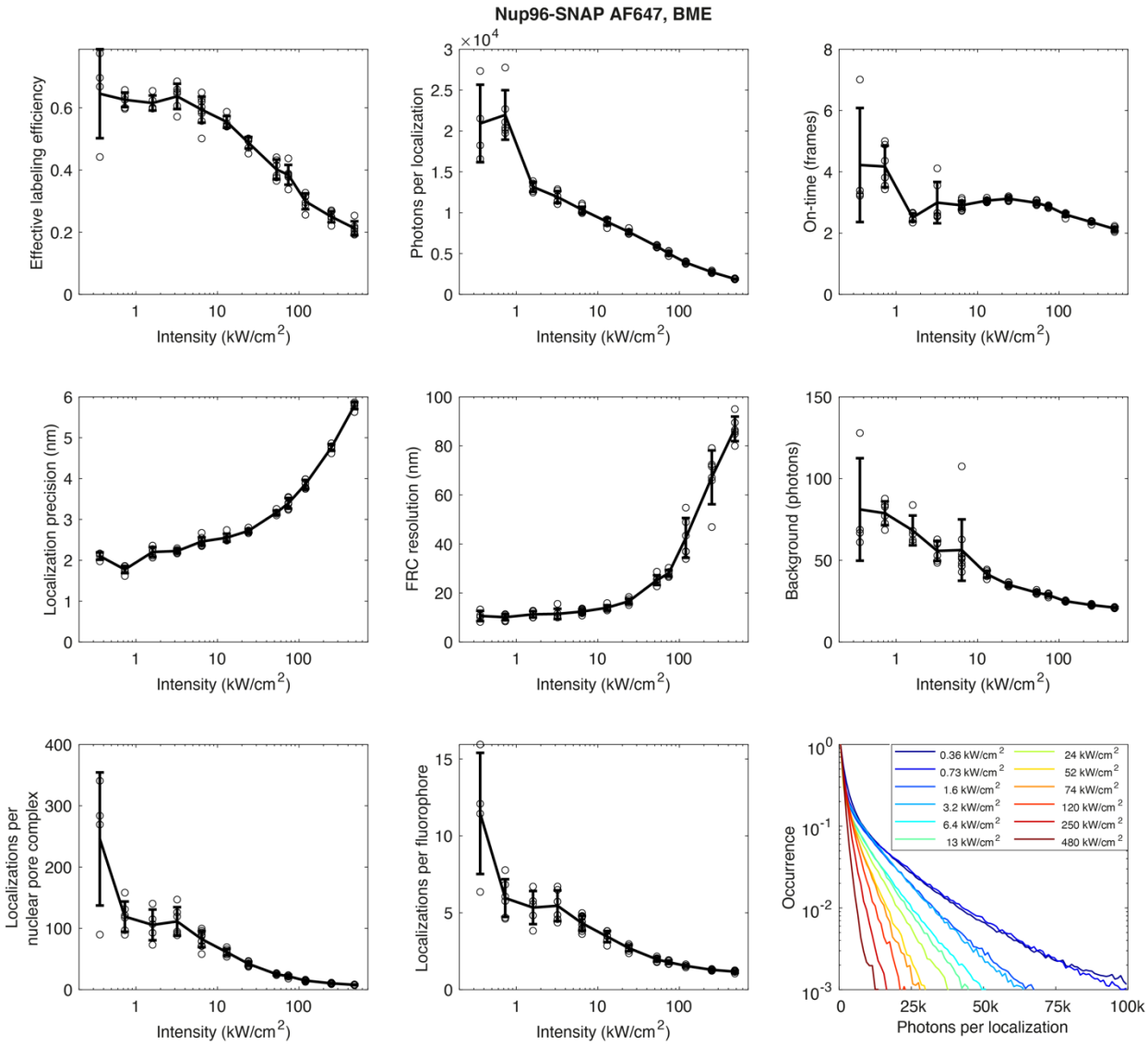

Nup96-SNAP-AF647 in 143 mM BME

Localization statistics for Nup96-SNAP labeled with BG-AF647 in glucose oxidase/catalase buffer, supplemented with 143 mM BME. For each intensity, the mean value ± standard deviation is shown over the data points representing individual cells. See Supplementary Table 1 for an overview about sample size and replicates and Supplementary Dataset 1 for detailed information about each measurement.

Supplementary Figure 3: Nup96-SNAP-AF647 in 35 mM MEA

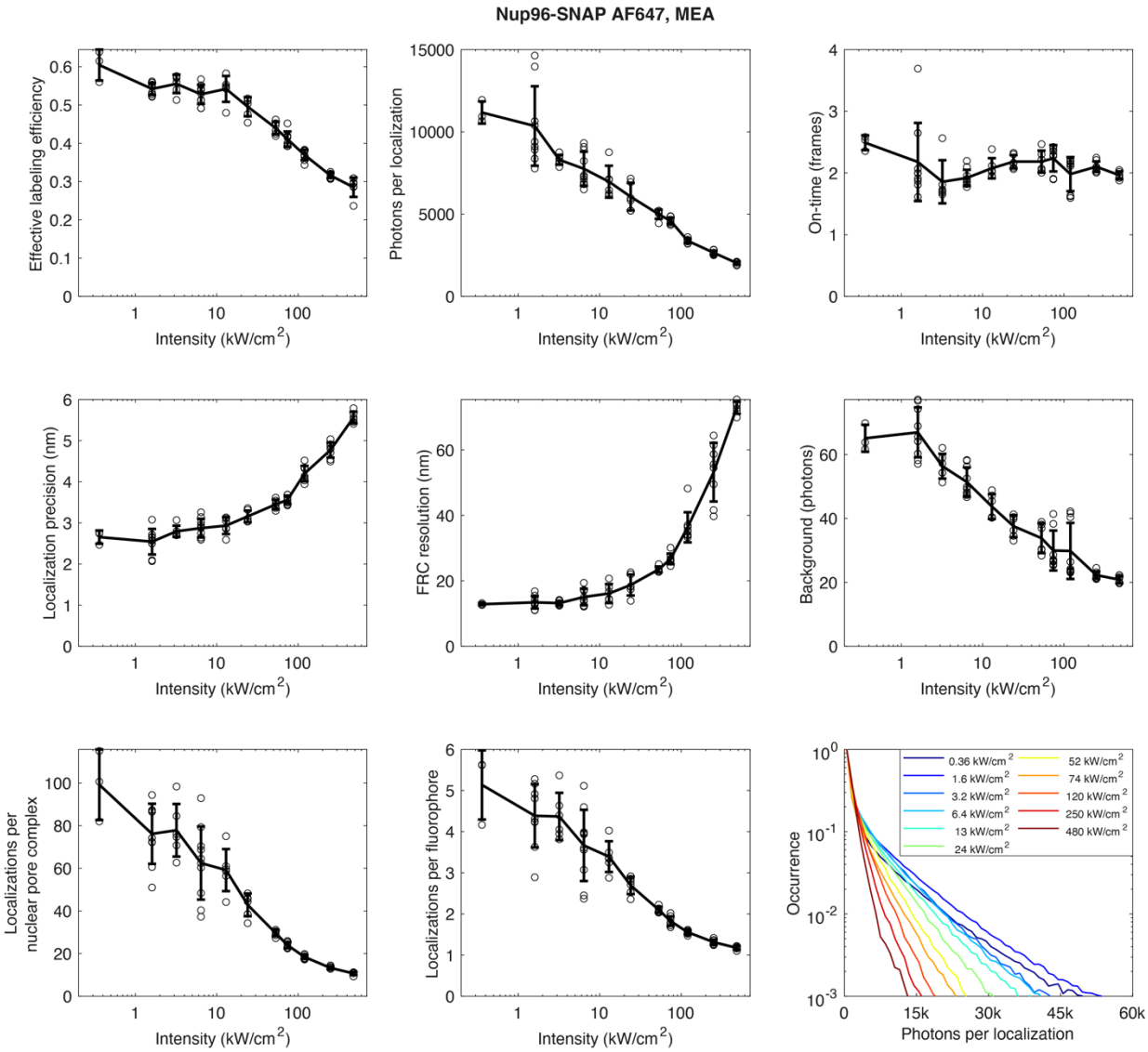

Nup96-SNAP-AF647 in 35 mM MEA

Localization statistics for Nup96-SNAP labeled with BG-AF647 in glucose oxidase/catalase buffer supplemented with 35 mM MEA. For each intensity, the mean value ± standard deviation is shown over the data points representing individual cells. See Supplementary Table 1 for an overview about sample size and replicates and Supplementary Dataset 1 for detailed information about each measurement.

Supplementary Figure 4: Nup96-mEGFP-AB-AF647 in 143 mM BME

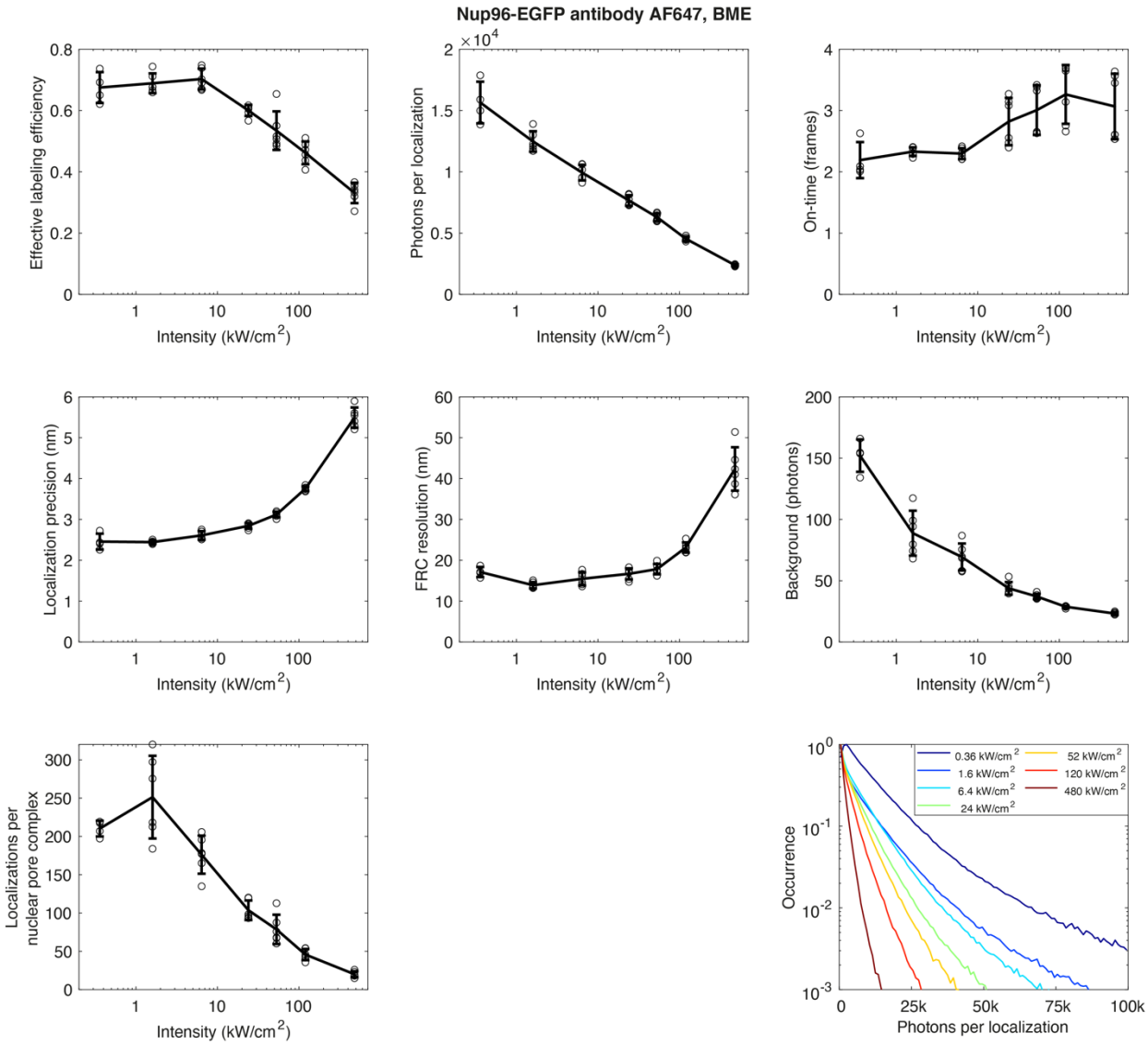

Nup96-mEGFP-AB-AF647 in 143 mM BME

Localization statistics for Nup96-mEGFP labeled with an anti-GFP antibody and a secondary antibody conjugated to AF647 in glucose oxidase/catalase buffer supplemented with 143 mM BME. For each intensity, the mean value ± standard deviation is shown over the data points representing individual cells. See Supplementary Table 1 for an overview about sample size and replicates and Supplementary Dataset 1 for detailed information about each measurement.

Supplementary Figure 5: Nup96-SNAP-AF647 in 143 mM BME + 48 % glycerol

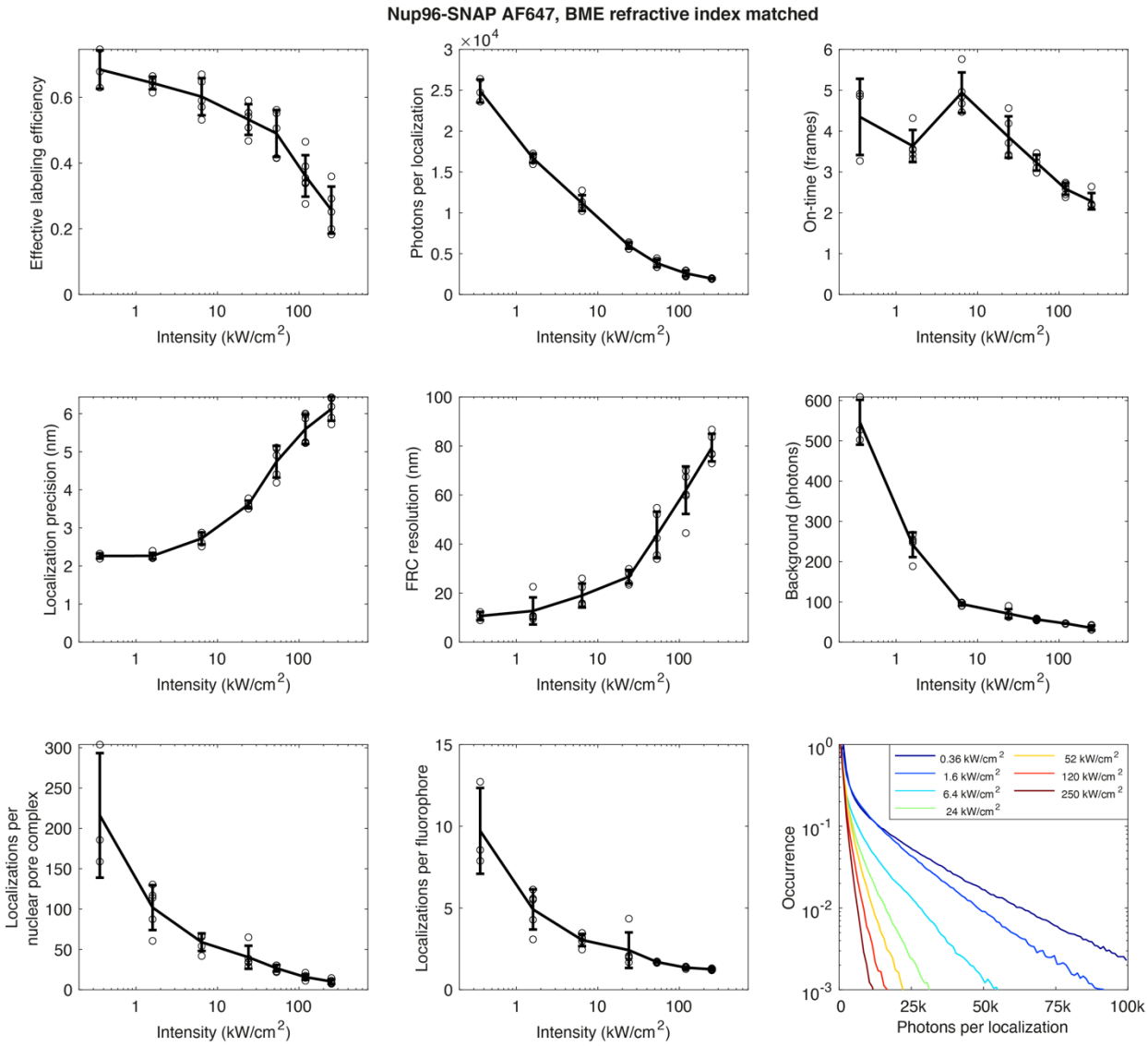

Nup96-SNAP-AF647 in 143 mM BME + 48 % glycerol

Localization statistics for Nup96-SNAP labeled with BG-AF647 in glucose oxidase/catalase buffer supplemented with 143 mM BME + 48 % glycerol for refractive index matching. For each intensity, the mean value ± standard deviation is shown over the data points representing individual cells. See Supplementary Table 1 for an overview about sample size and replicates and Supplementary Dataset 1 for detailed information about each measurement.

Supplementary Figure 6: Microtubule-AB-AF647 in 143 mM BME

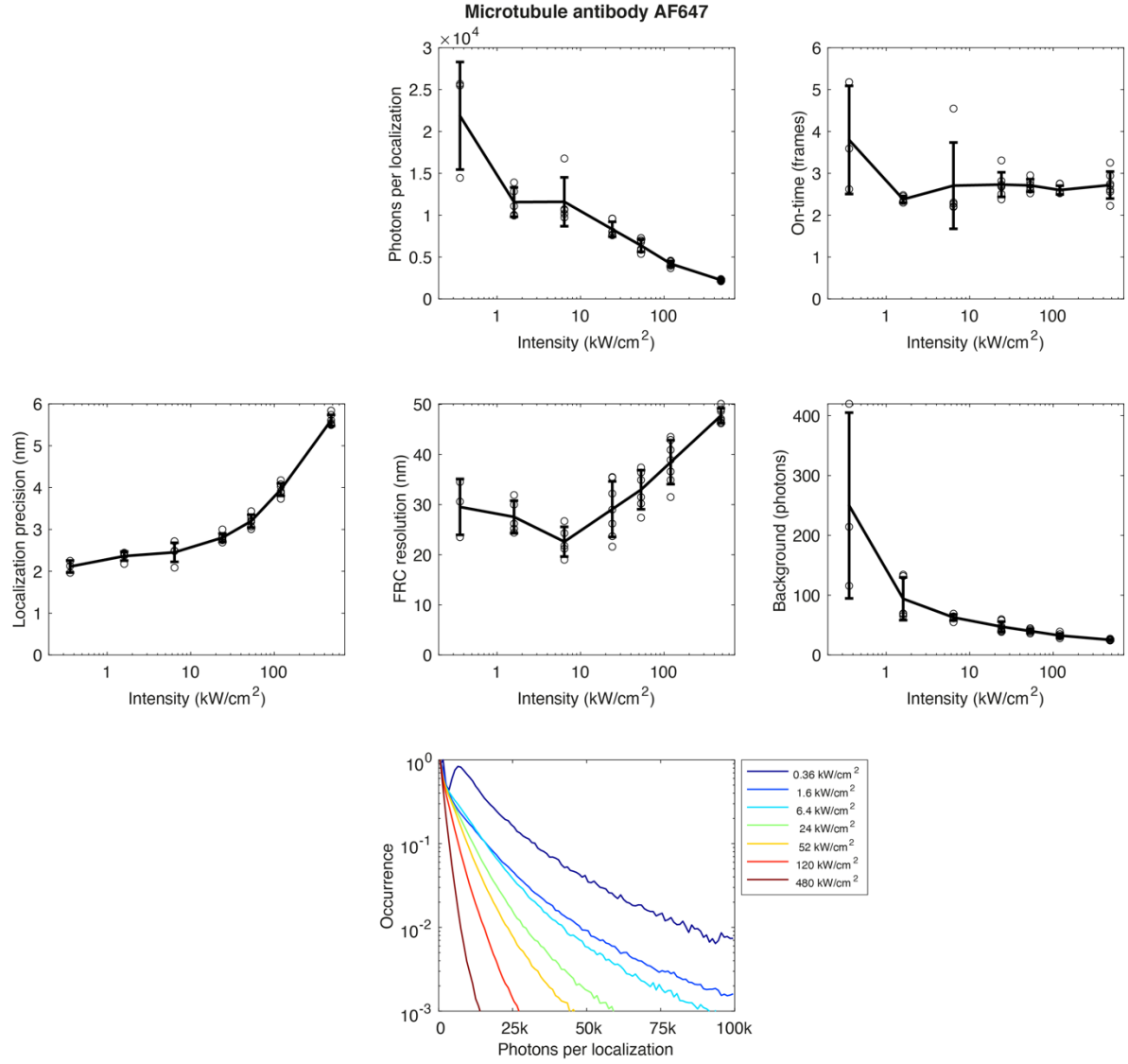

Microtubule-AB-AF647 in 143 mM BME

Localization statistics for Microtubules labeled with primary anti α-Tubulin antibodies and secondary antibodies conjugated to AF647 in glucose oxidase/catalase buffer supplemented with 143 mM BME. For each intensity, the mean value ± standard deviation is shown over the data points representing individual cells. See Supplementary Table 1 for an overview about sample size and replicates and Supplementary Dataset 1 for detailed information about each measurement.

Supplementary Figure 7: Nup96-mEGFP-NB-CF680 in 143 mM BME

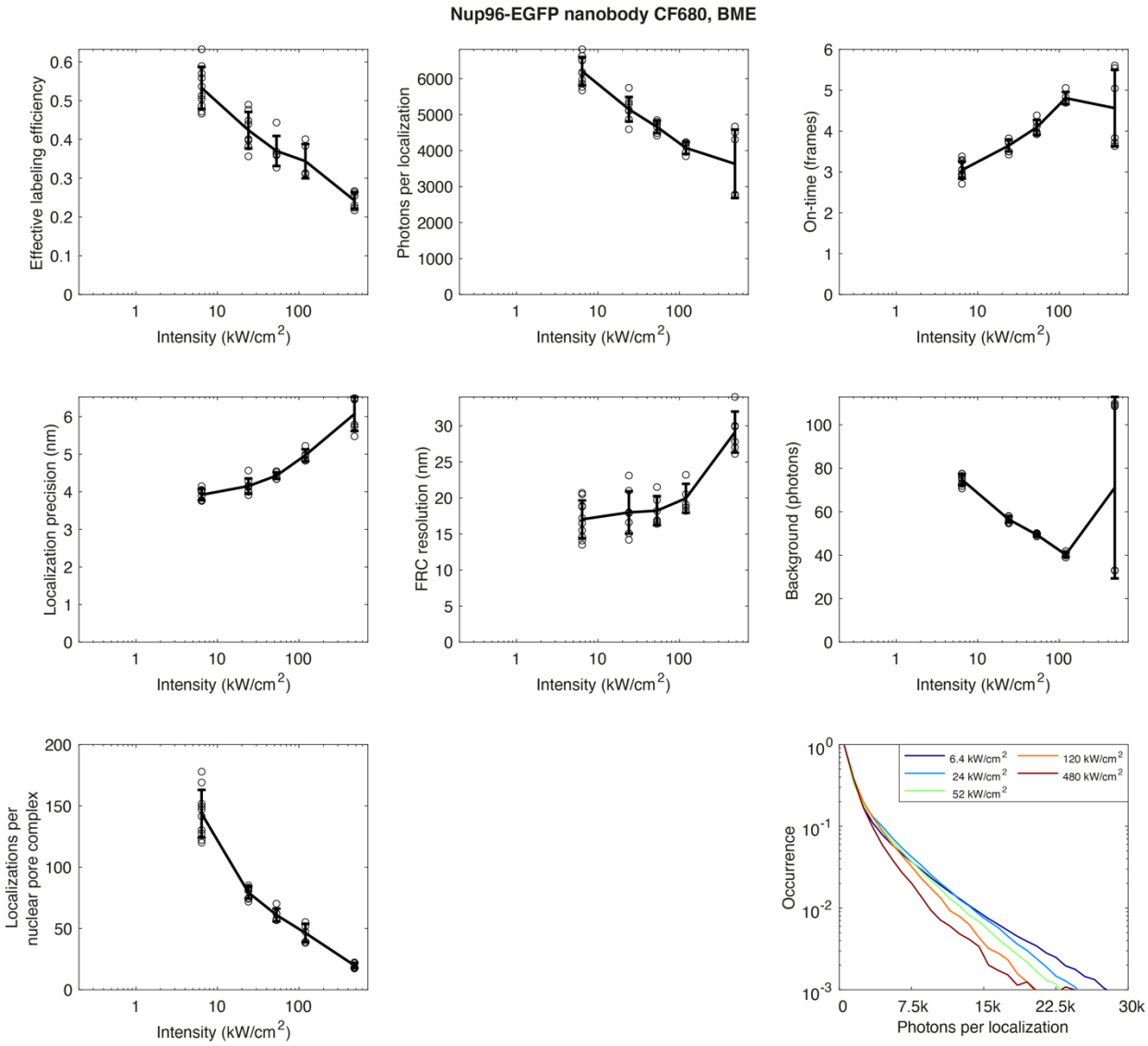

Nup96-mEGFP-NB-CF680 in 143 mM BME

Localization statistics for Nup96-mEGFP labeled with an anti-GFP nanobody coupled to CF680 in glucose oxidase/catalase buffer supplemented with 143 mM BME. For each intensity, the mean value ± standard deviation is shown over the data points representing individual cells. See Supplementary Table 1 for an overview about sample size and replicates and Supplementary Dataset 1 for detailed information about each measurement.

Supplementary Figure 8: Nup96-mEGFP-AB-CF660C in 143 mM BME

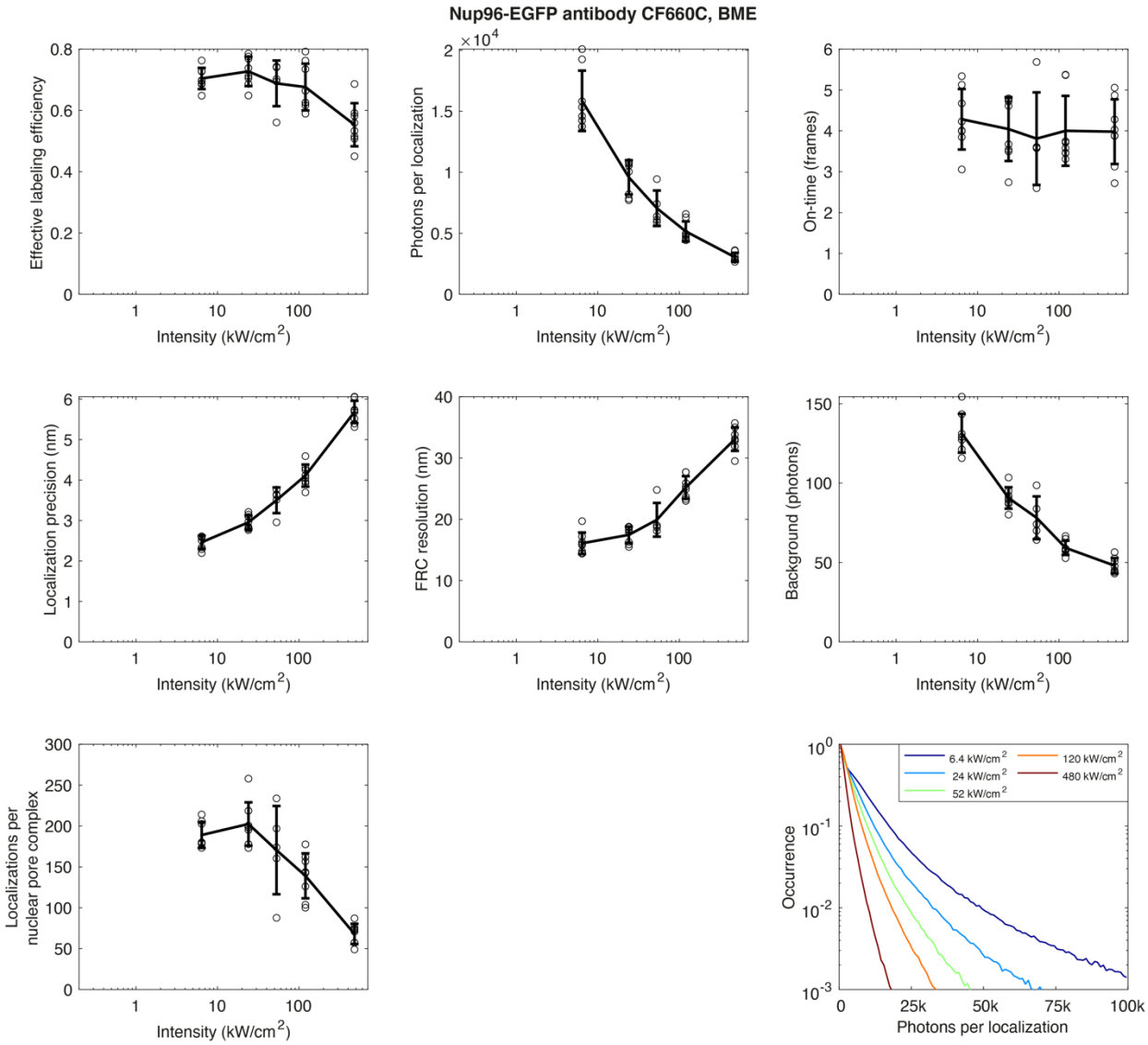

Nup96-mEGFP-AB-CF660C in 143 mM BME

Localization statistics for Nup96-mEGFP labeled with an anti-GFP primary antibody and a secondary antibody conjugated to CF660C in glucose oxidase/catalase buffer supplemented with 143 mM BME. For each intensity, the mean value ± standard deviation is shown over the data points representing individual cells. See Supplementary Table 1 for an overview about sample size and replicates and Supplementary Dataset 1 for detailed information about each measurement.

Supplementary Figure 9: Nup96-mEGFP-AB-Dy634 in 143 mM BME

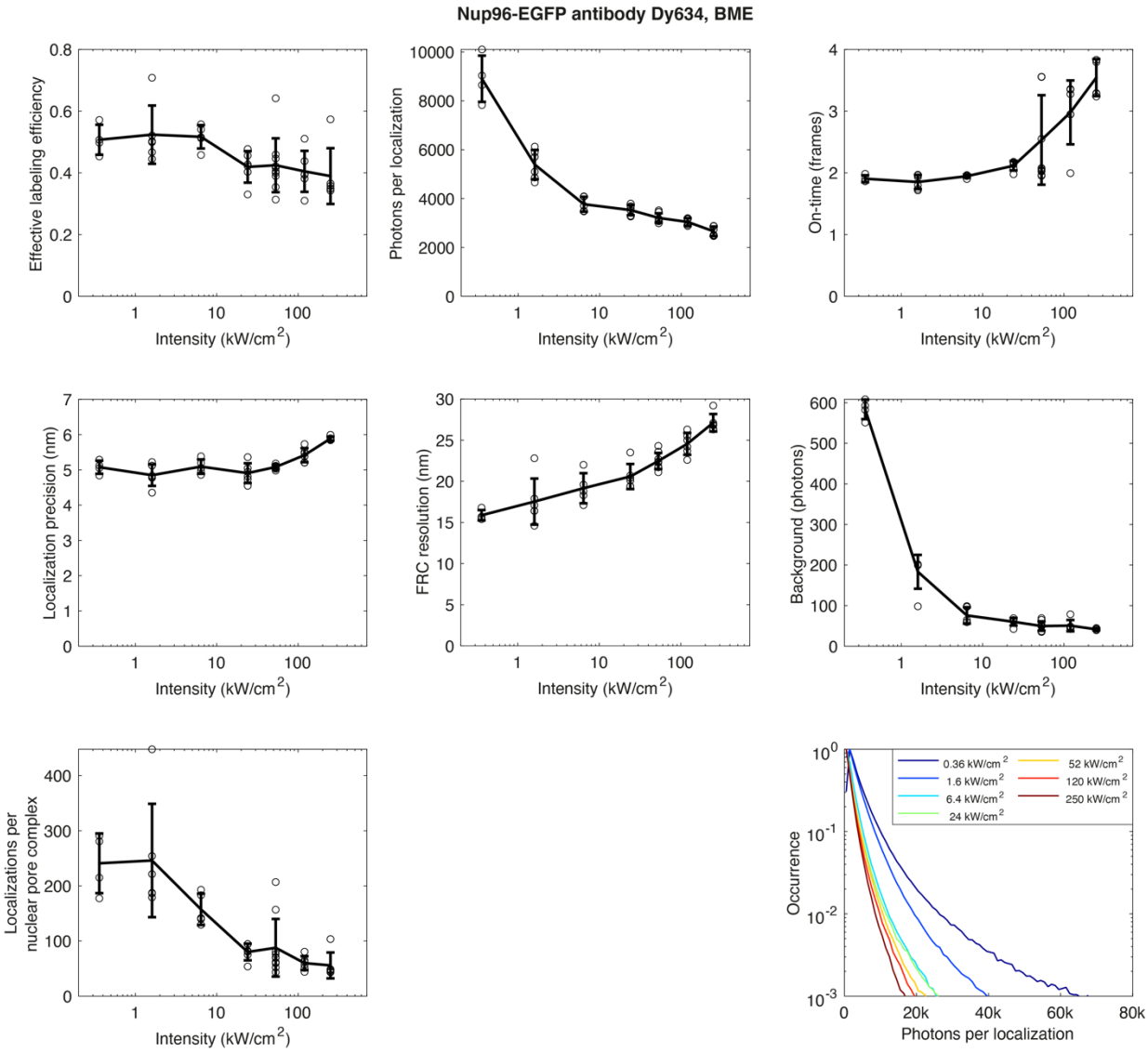

Nup96-mEGFP-AB-Dy634 in 143 mM BME

Localization statistics for Nup96-mEGFP labeled with an anti-GFP primary antibody and a secondary antibody conjugated to Dy634 in glucose oxidase/catalase buffer supplemented with 143 mM BME. For each intensity, the mean value ± standard deviation is shown over the data points representing individual cells. See Supplementary Table 1 for an overview about sample size and replicates and Supplementary Dataset 1 for detailed information about each measurement.

Supplementary Figure 10: Nup96-mMaple in 95 % D_2O

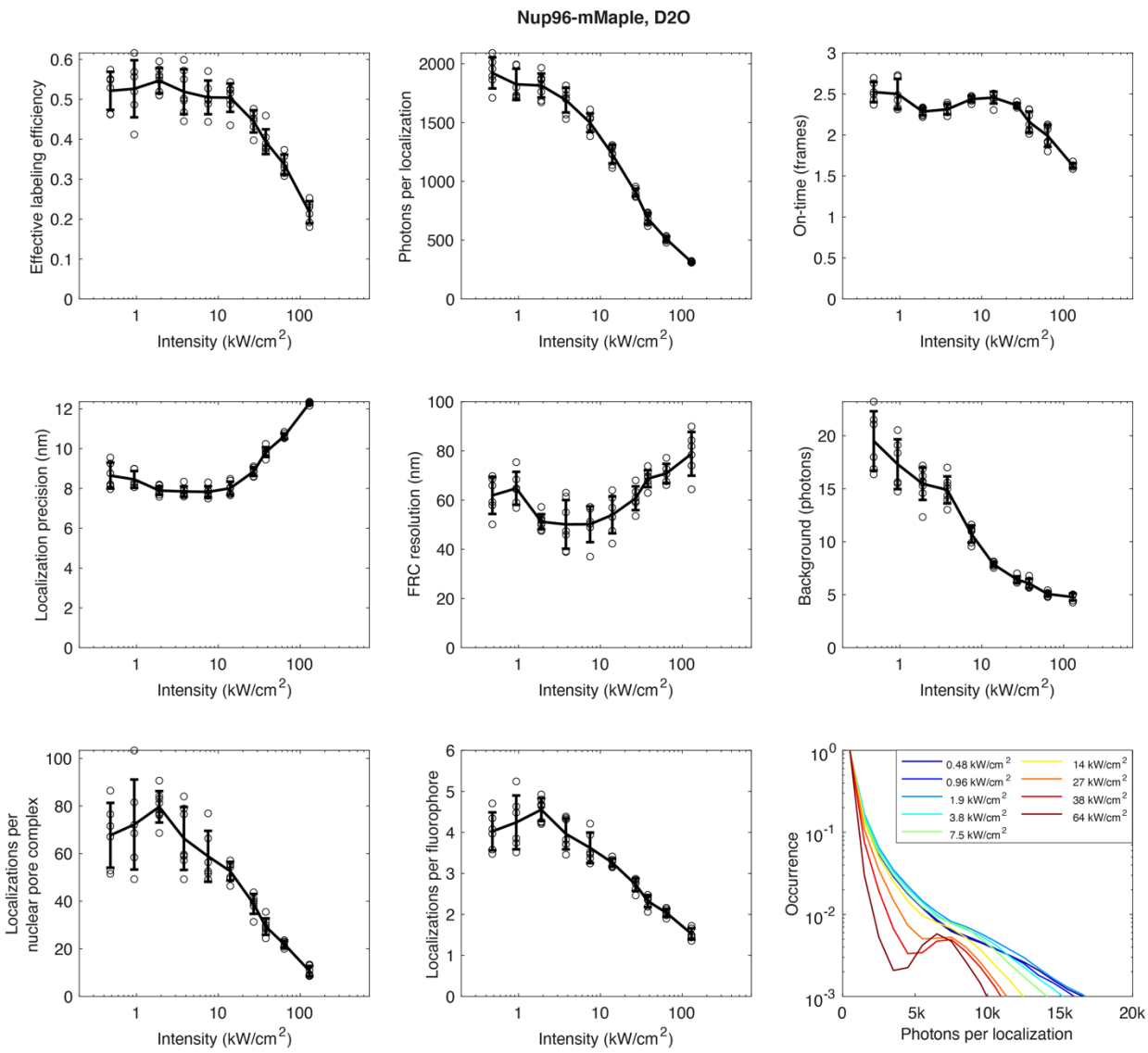

Nup96-mMaple in 95 % D_2O

Localization statistics for Nup96-mMaple in D_2O buffer. For each intensity, the mean value±standard deviation is shown over the data points representing individual cells. See Supplementary Table 1 for an overview about sample size and replicates and Supplementary Dataset 1 for detailed information about each measurement.

Supplementary Figure 11: Quantitative comparison of AF647 and CF660C

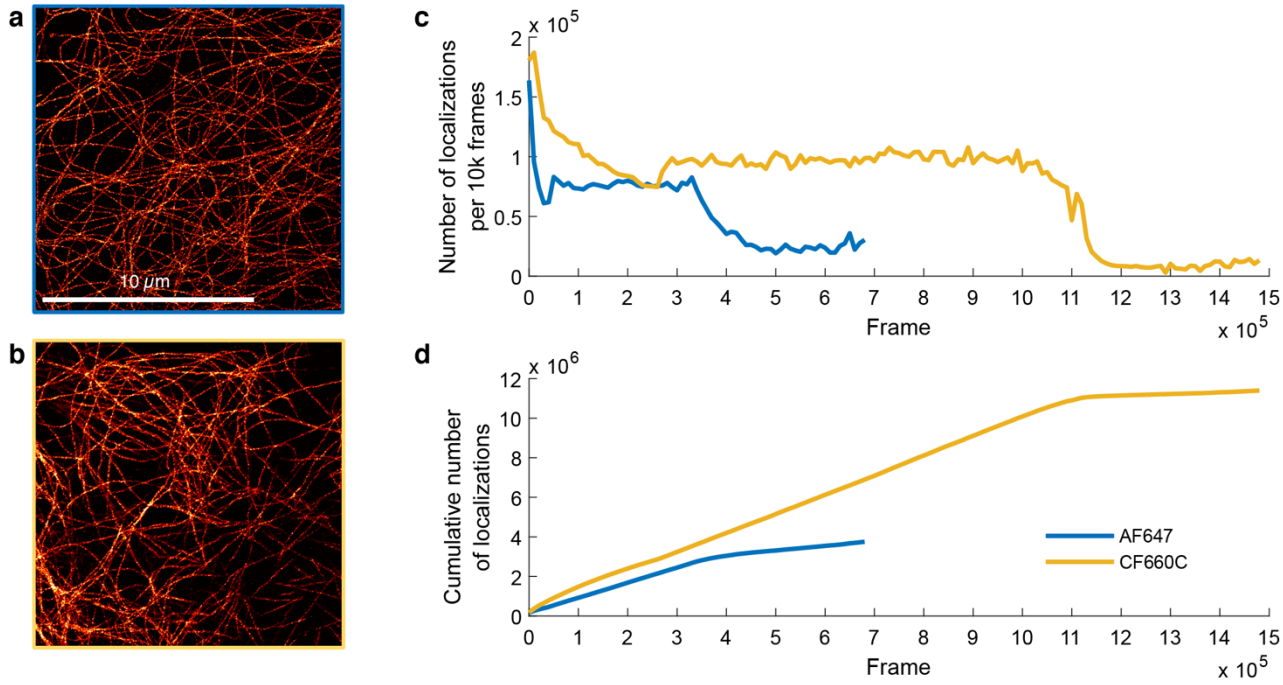

Quantitative comparison of AF647 and CF660C

Microtubules in U2OS cells were immunostained with AF647 (**a**) or CF660C (**b**) and imaged until bleaching of almost all fluorophores in the field of view. **c**,**d**, AF647 yields about 3,000,000 localizations in 350,000 frames, while CF660C yields about 10,000,000 localizations in 1,100,000 frames over the ROI. To keep the density of bright fluorophores (number of localizations per frame) constant, the number of active emitters was measured continuously and the UV laser power was increased gradually when the number of emitters fell under a pre-defined threshold. Once the UV laser power reached its maximum and almost all fluorophores were bleached, the number of localizations dropped and the acquisition was stopped shortly after. Representative data from $n_c = 2$ individual cells is shown for each condition from the same preparation (N = 1). Excitation intensity 24 kW/cm^2, Effective exposure time 7.5 ms.

Supplementary Figure 12: Custom-built microscope

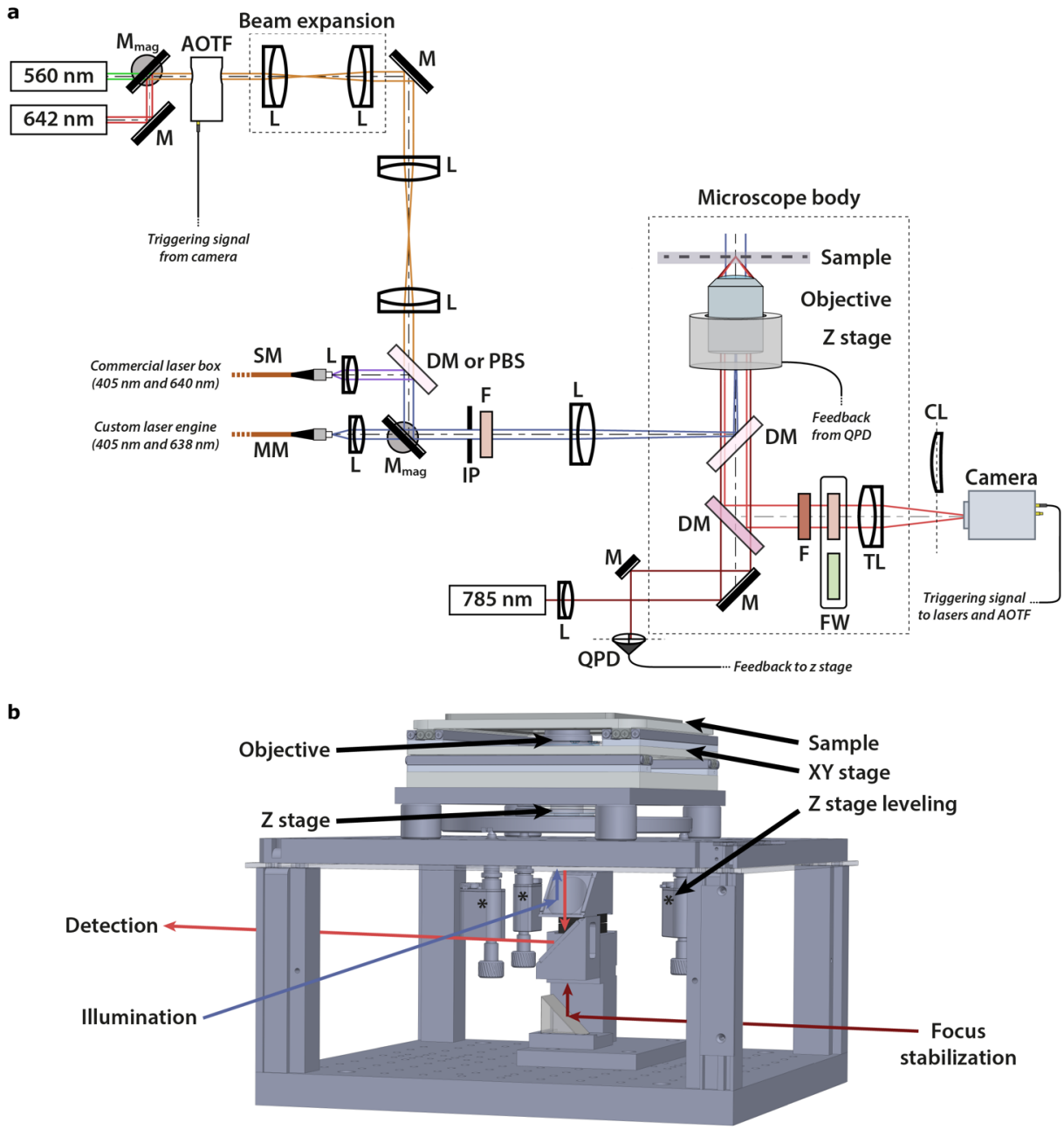

Custom-built microscope

(**a**) **Optical path** as described in the materials and methods section. Lasers are indicated by their emission wavelength. The microscope body and the beam expansion system are delimited by dashed boxes. AOTF: acousto-optic tunable filter, DM: dichroic mirror, CL: cylindrical lens, F: filter, FW: filter wheel, IP: image plane, L: lens, M: mirror, M_{mag}: mirror on a magnetic base, MM: multimode optical fiber, PBS: polarization beam splitter, QPD: quadrant photo-diode, SM: single-mode optical fiber, TL: tube lens. (**b**) **Computer-aided design rendering** of the custom microscope. Black arrows point to microscope elements, while colored arrows follow the optical beam paths of the focus stabilization, the illumination and the detection. Asterisks denote three piezoelectric stages used to level the z-stage.

Supplementary Note 1: Microscope setup

Microscope optics

All imaging, except for ratiometric two- and three-color imaging (see below), was performed on a custom built microscope described in the following (beam path in **Supplementary Figure 12**): The beams of 2 W lasers (F-04306-107 and F-04-306-102, MPB Communications) emitting at a wavelength of 642 nm or 560 nm, respectively, at constant power were guided through an acousto-optic tunable filter (AOTF) (Mod.n, AA Opto Electronic) and expanded by a telescope (either AC254-050-A f=50 mm and AC254-100-A f = 100 mm or ACN254-075-A f = -75 mm and AC254-250-A f = 250 mm, all Thorlabs). The lasers passed through a laser clean-up filter and were relayed in a 4f configuration (2 times AC508-250-A f = 250 mm, Thorlabs) to an additional plane conjugate to the image plane. An adjustable aperture was placed in this plane and closed such that just the camera region of interest (ROI) was illuminated. Either just before this intermediate image plane using a dichroic mirror (DMLP425, Thorlabs), or directly after the expanding telescope using a polarizing beamsplitter cube (PBS251, Thorlabs), the 2 W lasers were combined with the collimated (AC254-060-A f = 60 mm, Thorlabs) output of a laser box (iCHROME-MLE-L-D, Toptica). The laser box emitted laser light at a wavelength of 405 nm at 50 mW maximum power, which was used for active photo-switching, and 640 nm at 80 mW maximum power, which was used for fluorescence excitation alternatively to the 2 W laser.

Either an achromatic lens (AC254-150-A f = 150 mm, Thorlabs) or a pair of two achromatic lenses in Plössl-configuration (2x G322355000, f = 500 mm, Qioptiq) and the objective lens (100x/NA1.35 silicone oil immersion, Olympus, for whole-cell 3D imaging and for Nup96 single color 3D imaging; 100x/NA1.5 oil immersion, Olympus, for live-cell imaging; or 100x/NA1.35 oil immersion, Olympus, for single color 2D imaging) image the intermediate image plane in 4f configuration to the sample to achieve widefield epi-illumination.

One dichroic mirror (ZT405/488/561/640rpc TIRF, Chroma) was used to separate fluorescence excitation and emission. The fluorescence emission was filtered by a short pass filter (FESH0750, Thorlabs) to block the focus-lock laser (see below). A filter wheel was used to select filters based on the experiment: mMaple emission was filtered using a combination of two filters (600/60, Chroma, and 568 Edge Basic, Semrock), AF647 emission was filtered using a combination of two bandpass filters (FF01-767/37, Semrock, and 700/100m, Chroma), CF660C and CF680 emission was filtered using a bandpass filter (FF01-697/58, Semrock) for intensity dependent measurements, but for whole-cell 3D imaging, CF660C emission was filtered using a different bandpass filter (ET685/70m, Chroma).

The tube lens (TTL100-A f = 100 mm, Thorlabs) focused the image plane onto a back-illuminated sCMOS camera (Edge 4.2bi, PCO) at a projected pixel width of 117 nm. For astigmatic 3D imaging, we placed a cylindrical lens (plcx f = 1500 mm, VM-TIM) between the tube lens and the camera.

The microscope contained a custom focus stabilization system: A dichroic mirror was used to couple in a 785 nm infrared laser (Toptica) and focus it at the periphery of the back-focal plane. The back reflected part of the infrared laser from the coverslip-medium interface was guided to a four-quadrant photodiode to read out the relative z-position between objective lens and coverslip for active z-drift compensation.

For whole-cell 3D imaging, the sample was illuminated with a low-cost laser engine described elsewhere . In brief, the light emitted from laser diodes at 405 nm (dl-7146-301s, Sanyo) and 640 nm (HL63193MG, Ushio) was spatially combined and coupled into a square multi-mode fiber (M103L05, Thorlabs). The fiber output was imaged (AC127-019-A, Thorlabs) to the intermediate image plane described above to achieve flat illumination over a ROI of about 40 µm x 40 µm.

Ratiometric two- and three-color imaging was performed on a different custom-built microscope described elsewhere in detail [1-3]. For ratiometric emission splitting, we used an imaging-grade dichroic beamsplitter (T665lpxr, Chroma) in combination with a bandpass filter (ET685/70m, Chroma) for the transmitted channel and a bandpass filter (FF01-676/37, Semrock) for the reflected channel. The type of fluorophore was assigned to the individual localizations by the intensity ratio in the two channels simultaneously imaged side by side on the same EM-CCD camera (Evolve512D, Photometrics, or Evolve512, Photometrics).

Laser intensity calibration

The Gaussian intensity profile of the lasers was observed from fluorescence in the sample plane and a Gaussian function was fitted to reveal the characteristic width in the sample. We selected the central region in which the intensity varied from 80 % to 100 % of the peak intensity. We placed an iris in the conjugate image plane and centered it to the Gaussian illumination profile. We then closed it to the diameter corresponding to the 80 % to 100 % of the peak intensity in the central region. The laser power was then measured just before entering the objective back aperture. Dividing the power by the area of this central region gives the mean intensity in the region of interest. The transmission efficiency of the objective lens was additionally corrected for. Alternatively, the laser power was directly measured at the exit pupil of the objective lens. To adjust the intensity between measurements, we temporarily placed a power-meter (Thorlabs) in the beam path at a reference position and used the ratio of the power at the reference point and the objective lens to calculate the respective intensities. For excitation emitted from a multi-mode fiber, we followed a similar procedure using an aperture in the intermediate image plane that we closed to a defined area in the sample plane and measured the power at the objective lens to find the mean intensity in the region of interest.

Microscope control and electronics

Data was recorded and hardware was controlled via the software package Micro-Manager[4] (version 1.4.22 or 2.0.0-gamma) in ImageJ (Fiji) using a custom plugin[5]. The camera sent a

trigger signal during simultaneous exposure of all lines to an FPGA board (Mojo, Alchitry). The FPGA board outputs were controlled via Micro-Manager. To trigger the AOTF output, the FPGA board sent a TTL output synchronized to the camera exposure. The voltage was scaled via a custom-built circuit board to 0 – 10 V and connected to the AOTF blanking input or connected to the laser drivers. The AOTF channel input was directly connected to a voltage supply that allows for setting the desired laser power. We used an oscilloscope connected with its first channel to the camera trigger output and with its second channel connected to a power meter of which the sensor was placed in the laser beam. The oscilloscope measurement confirmed that the laser power output of the AOTF and the camera exposure were in synchronization, while the lag in the laser signal was about 10 µs, which corresponds to an error below 3 % in the estimated laser exposure per frame even for the shortest effective exposure time of 375 µs.

The 405 nm laser was run at constant power but pulsed in synchronization with the beginning of each frame exposure. The pulse width was dynamically adjusted by the custom-written Micro-Manager plugin to achieve a desired number of active emitters per frame until almost all emitters were bleached.

Supplementary Note 2: Model for fluorophore blinking and bleaching for organic dyes in blinking buffer

Here, we considered two simple three-state models that we extended to include photobleaching (**Extended Data Figure 2**). Model 1 was inspired by work by van der Linde et al.[6] and Lin et al.[7], which suggests that off-switching occurs from the triplet state by interaction with the thiol. Model 2 is a simplified version of a model by Dempsey et al.[8], which describes off-switching as a light-induced reaction of the bright state with the thiol. We modeled bleaching as a light-dependent process from the triplet state (which is many orders more long-lived than the excited singlet state under oxygen depletion). In addition, we considered that additional bleaching can occur during light-induced activation of the fluorophores, either by UV or the excitation light.

***Numerical solution of partial differential equations*.** We translated the models in **Extended Data Figure 2** to partial differential equations (PDEs) and solved them numerically using Mathematica (Wolfram research). We used as a boundary condition that all fluorophores are in the bright state at $t = 0$. The rate constants k_{bt}, k_{tb}, k_{td} were taken from Lin et al.[7], the remaining rate constants were varied manually to obtain similarity with the data. From the temporal evolution of the fraction of fluorophores in the bright state $B(t)$ and the bleached state $X(t)$ we estimated:

a) The number of photons per localization as:

$$\text{Photons} \sim \int_0^{tx} B(t) I \, dt,$$

with $tx = 10\ t_{exp}$, the camera exposure time $t_{exp} \cdot I = 0.176\ \text{s kW/cm}^2$, and the excitation intensity I.

b) The number of localizations per fluorophore as the total number of photons per fluorophore divided by the number of photons per localization:

$$\text{blinks} = \int_0^\infty B(t) I \, dt / \text{Photons}.$$

c) The labeling efficiency as:

$$LE = 1 - X(t_{\text{offswitch}}),$$

with the off-switching time $t_{\text{offswitch}} \cdot I = 30 \text{ s kW/cm}^2$.

d) The on-time as the time t where $B(t) == 0.5$, i.e. where half of the fluorophores were switched off.

Monte Carlo simulations. To compare our models better to the actual experiment, we performed Monte Carlo simulations on $N = 100\,000$ fluorophores per intensity value, using the same transition rates as for the PDE model. At $t = 0$ a fluorophore starts in its bright state. Then, for every possible transition to another state we draw an exponentially distributed random number (lifetime of the state) with a mean corresponding to the inverse transition rate. The transition corresponding to the lowest lifetime is the transition that occurs. In this way, we iteratively calculated states and transition times until the fluorophore is bleached. From the time of the transitions to and from the bright state, we calculated the frames in which a fluorophore is in its bright state. In a second step we performed merging of fluorophores and filtering as in our actual experiments.

Simulating the effect of varying exposure times

Our workflow performs realistic simulations of dye blinking and image formation on the camera.

In a first step, we modeled the positions and intensities of fluorophores in each frame. Fluorophores are defined by their average on-time t^{on} and the average fluorescence intensity I (measured in detected photons per time unit). a) we positioned the fluorophores in 3D at the protein positions in the nuclear pore complex and positioned hundreds of NPCs on a grid with additional random offsets in x,y, and z and tilts. b) for each fluorophore k we drew a random number for the time point $t_{d\to b}$ in which it is switched on. c) we drew a random number t_k^{on} from an exponential distribution (mean t^{on}) to determine its on-time. d) we defined the time points of the camera frames as multiples of the exposure time. e) a fluorophore was assigned a photon number N_k^f in each frame f that it was in its bright state. N_k^f is equal to the intensity I times the fraction of the frame that the fluorophore is in its bright state.

In a second step we simulated the camera frames using a symmetric 3D Gaussian PSF model for simplicity: a) For each frame f we rendered each fluorophore k as a 2D Gaussian function with a size $\sigma(z) = \sigma_0\sqrt{1 + (z - z_0)^2/z_R^2}$, with z_0 the focal position and z_R the divergence. The integrated intensity was set equal to N_k^f. b) We assumed a constant background intensity, and thus added a background proportional to the exposure time to each pixel. c) We applied pixel-wise Poisson noise with a mean equal to the intensity value of the pixel. d) To simulate the sCMOS camera used in this study, we added additional Gaussian read noise.

Simulated camera images were then fitted and analyzed in the same way as experimental data.

Supplementary Note 3: Software guide for quantitative SMLM analysis using SMAP

Note: This software guide is largely based on a manual published earlier (as Supplementary Information to https://doi.org/10.1038/s41592-019-0574-9) but has been updated to reproduce the workflow we used for the quantitative SMLM analysis in this work, based on the example data provided.

Example data of Nup96-SNAP-BG-AF647 for the excitation intensities of 0.73 kW/cm², 6.4 kW/cm² and 250 kW/cm² can be downloaded from: https://rieslab.de/#software.

Installation of SMAP (about 30 minutes)

Requirements

1. MATLAB newer than 2016a, explicitly tested with MATLAB 2019a. Toolboxes: Optimization, Image processing, Curve fitting, Statistics and Machine Learning. Optional: Parallel Computing
2. Mac or Windows
3. For GPU fitting: Windows, NVIDIA graphics card. CUDA driver (recommended: version 7.5).

Installation

1. Clone git repository:
    a. Use Terminal (MacOS) or Cmd (Win). Use cd to navigate to the target directory. (e.g. *cd git*)
    b. Type:
    git clone https://github.com/jries/SMAP
    and type in your username and password for your git account.
    c. Change to the “develop” branch. Type:
    git checkout develop
    d. Type:
    git pull
2. Follow the instructions in SMAP/Documentation/Manual/SMAPStep-by-StepGuide.md

Fitting of raw data in SMAP

Starting SMAP (about 1 minute)

1. Start MATLAB
2. Change the MATLAB current folder to the SMAP root directory.
3. Type: SMAP
    The SMAP main GUI will open.

Fitting (about 5 minutes per dataset, depending on the system)

Note: If fitting of the raw data is not desired, pre-fitted "…_sml.mat" files are provided and can be directly loaded into SMAP in the tab [File] by clicking the load button and selecting the dataset. In this case, skip the fitting step and go directly to the processing.

1. Go to the **[Localize]** tab.
2. If not set already, choose the workflow fit_fastsimple by clicking on **Change**.
3. In the **[Input Image]** tab click on load images and select the raw data tiff file (the first one in case it is a large stack or the frames are saved as individual images).
4. Switch to the **[Fitter]** tab and choose the "*PSF free*" fitter from the drop-down menu.
5. Switch to the **[Peak Finder]** tab and choose the threshold algorithm for the peak finding from the drop-down menu. We use "*dynamic (factor)*" with a value of 1.5.
6. Change the *preview mode* to "image", change the number next to the slider to 1000 and click on **Preview**. A window will open which shows the detected peaks and their fitted coordinates.
7. Click on **Localize** to start the fitting. Depending on the used computer and the raw data, this step can take a few minutes. On the tested system (i5-3570K CPU, GeForce GTX 660 Ti GPU, 32 GB memory), fitting 50,000 frames of 128 x 128 pixel takes about 180 seconds.
8. Once all the raw data is fitted, a *_sml.mat file containing the fitted positions and all associated information is automatically saved.

Processing of localizations

Localization filtering and image rendering (about 5 minutes per dataset)

Before further analysis, the image must be filtered to exclude incorrect localizations. This is achieved by setting boundaries for the parameter localization precision, PSF size, frames and likelihood. Furthermore, the colormode is changed to color-code localizations based on their background.

1. Click the button **OV -> filter**.
2. In the table at the top of SMAP, select the likelihood-filter *LLrel*. Set the filter lower bound to the value -2.5 exclude the accumulation of localizations (shown as a green bar) on the left side of the histogram.
3. Activate the *LLrel*-filter by checking *filter*.
4. Go to [Render].
5. In *Filter fields*, set the *locprec* upper bound (right value) to 10*, PSF xy* upper bound (right value) to 160*, frame* lower bound (left value) to 1000*.*
6. Change Colormode to field and bg.
7. Change *LUT* to *jet*.
8. Change the *c range* lower bound (left value) and upper bound (right value) depending on the dataset from the example raw data (These values only influence the rendering but not the quantitative analysis):
    a. For 0.73 kW/cm², use about 45 to 75.

    b. For 6.4 kW/cm² use about 30 to 55.
    c. For 250 kW/cm2 use about 20 to 30.
9. Change *contrast* to -2.5
10. Click **Render**.

Drift correction (about 2 minutes per dataset)

1. Go to tab **[Process]**, sub-tab **[Drift],** *drift correction X,Y,Z.*
2. Click on **Run** to start the drift correction with the default parameters.

Setting the ROI (about 1 minute per dataset)

We only evaluate localizations within a ROI where the laser intensity varied from 80 % to 100 % of the peak intensity. Due to the Gaussian illumination profile of our microscope, this corresponds to a circle of 10,000 nm diameter.

1. In the **ROI** panel above the filter -> OV button, click the elliptical symbol.
2. Draw a circular ROI of 10000 x 10000 nm centered to the illumination profile, which can be easily assessed by the localizations color coded for the background (higher background in the center).

Segmentation of NPCs inside the ROI (about 15 minutes per dataset)

The filtered and drift corrected super-resolution image will be automatically segmented for the individual nuclear pore complexes (NPCs).

1. Make sure the circular ROI is still drawn in the image window.
2. Go to the **[ROIs]** tab in the SMAP main GUI.
3. In the **[Settings]** sub-tab, click **show ROI manager**. A window will open.
4. In the SMAP main GUI, click **redraw all**.
5. Go to sub-tab **[Segment], run** the *makeCellGrid* plugin.
6. Go to sub-tab [Settings], click Redraw all.
7. Go to sub-tab **[Segment], run** the *segmentNPC* plugin. Used parameters for NPC segmentation are
    a. cutoff: 0.06,
    b. diameterNPC: 105,
    c. rim: 20.
    d. Check the box saveon before running the plugin.
8. In the upper row of the SMAP main GUI, navigate to **Plugins -> ROIManager -> Segment ->UseSitesInROI**. A window will open, click the **Run** button.
9. Change to the ROIManager window and click the button **upd**. The list will update and sites outside the ROI will be marked by a "–" as their last character.
10. In the SMAP main GUI, go to the **[ROIs]** tab, sub-tab **[Helper]**. Change the dropdown menu next to **1st** sort to **Use** and click the **Run** button.
11. Change back to the ROIManager window and have a look at the sites list. All unused site (marked by a "–" as their last character) will come first, all used sites (marked by a "+" as their last character) will come last. To mark all unused sites in

the list, click the first unused site, scroll down, hold the **Shift** key and click the last unused site. Then click the **Remove** button. Now only sites inside the circular ROI should be left and will be considered for further analysis.

12. In the SMAP main GUI, go to the **[ROIs]** tab, sub-tab **[Evaluate]**. Click the **add module** button. A window will open. Select *NPCsegmentCleanup* in the list and click **OK**.
13. In **[Evaluate]** check only *NPCsegmentCleanup*. Click on *NPCsegmentCleanup* to display its settings on the right hand side. Change
    a. min localizations to 5,
    b. use default parameters else.
14. Run the plugin by checking *evaluate on* (*display* can be unchecked to increase processing speed) and a click on **redraw all**. This step can take several minutes.
15. Change to the ROIManager window and click the button **upd**. The list will update and sites unsuccessful during the *NPCsegmentCleanup* quality check will be marked by a "–" as their last character.
16. In the SMAP main GUI, go to the **[ROIs]** tab, and the **[Helper]** subtab. Change the dropdown menu next to **1st** sort to **Use** and click the **Run** button.
17. Change back to the ROIManager window. Again, click the first unused site, scroll down, hold the **Shift** key and click the last unused site. Then click the **Remove** button.

Quantitative analyses

Determining effective Labeling efficiency (about 10 minutes per dataset)

1. Under tab **[ROIs]**, sub-tab **[Evaluate]** uncheck *NPCsegmentCleanup* and check *generalStatistics*
2. Use **[add module]** to add the plugin *NPCLabelingQuantify_s.* Unclick the **display** checkbox. Run the plugin by clicking the **redraw all** button. This step can take several minutes.
3. Go to tab **[Analyze]**, sub-tab **[NPC]**.
4. Select *NPCLabelingEfficiency*. Standard parameters are optimized for evaluation of Nup96 effective labeling efficiency. Start the plugin by **Run**.
5. A window opens after the plugin is finished. The effective labeling efficiency and the error is written in the tab **[corners].** Additionally, results of the plugin are automatically saved to the clipboard to paste them into a spreadsheet.

Anticipated results from the example raw data, slightly dependent on the position of the circular ROI:

- 0.73 kW/cm²: Effective labeling efficiency ~63.6 %
- 6.4 kW/cm²: Effective labeling efficiency ~62.0 %
- 250 kW/cm²: Effective labeling efficiency ~24.3 %

Analysis of fluorophore photophysics (about 1 minutes per dataset)

1. Make sure the circular ROI is still drawn in the image window.
2. Go to tab **[Analyze]**, sub-tab **[measure]** in the SMAP main GUI.
3. Select *Statistics.* Change the lower bound (first value) of the *photon range* to 200.
4. Start the plugin by **Run**.
5. A window opens, showing various photon statistics. Additionally, results of the plugin are automatically saved to the clipboard to paste them into a spreadsheet.

Anticipated results from the example raw data, slightly dependent on the position of the circular ROI:

- 0.73 kW/cm²: Photons <P_all> ~20,000; locprec median ~1.8 nm
- 6.4 kW/cm²: Photons <P_all> ~10,000; locprec median ~2.4 nm
- 250 kW/cm²: Photons <P_all> ~3,000; locprec median ~4.6 nm

Saving the result

1. Go to the SMAP main GUI, tab **[File]**.
2. Click the **Save** button.

Loading a saved result

1. Go to the SMAP main GUI, tab **[File]**.
2. Check load GIU Parameters and check restore ROI.
3. Click load and select the file.

References for Supplementary Information

1 Thevathasan, J. V. *et al.* Nuclear pores as versatile reference standards for quantitative superresolution microscopy. *Nature Methods* **16**, 1045-1053 (2019).

2 Mund, M. *et al.* Systematic Nanoscale Analysis of Endocytosis Links Efficient Vesicle Formation to Patterned Actin Nucleation. *Cell* **174**, (2018).

3 Deschamps, J., Rowald, A. & Ries, J. Efficient homogeneous illumination and optical sectioning for quantitative single-molecule localization microscopy. *Opt Express* **24**, (2016).

4 Edelstein, A., Amodaj, N., Hoover, K., Vale, R. & Stuurman, N. Computer control of microscopes using μManager. *Curr Protoc Mol Biol* **92**14.20.1-14.20.17 (2010).

5 Deschamps, J. & Ries, J. EMU: reconfigurable graphical user interfaces for Micro-Manager. *bioRxiv*, 2020.2003.2018.997494, doi:10.1101/2020.03.18.997494 (2020).

6 van de Linde, S. *et al.* Photoinduced formation of reversible dye radicals and their impact on super-resolution imaging. *Photochem Photobiol Sci* **10** (2011).

7 Lin, Y. *et al.* Quantifying and Optimizing Single-Molecule Switching Nanoscopy at High Speeds. *PLOS ONE* **10**, e0128135 (2015).

8 Dempsey, G. T. *et al.* Photoswitching Mechanism of Cyanine Dyes. *Journal of the American Chemical Society* **131** (2009).

Additional Supplementary Material

Supplementary Video 1: Whole-cell 3D, YZ reconstruction
YZ slice translation through the cell shown in Figure 2a. Scale bar, 10 µm.

Supplementary Video 2: Whole-cell 3D, 3D reconstruction
3D reconstruction of a part of the cell shown in Figure 2a. Scale bar, 10 µm.

Supplementary Video 3: Whole-cell 3D, mitotic cell
3D reconstruction of the mitotic cell and surrounding cells as shown in Extended Data Figure 5. Scale bar, 10 µm.

Supplementary Video 4: Three-color 3D data on the NPC
3D reconstruction of the three-color ratiometric image of the nuclear pore complexes shown in Extended Data Figure 6. Colors: Red – Nup96-SNAP-AF647, Green – ELYS immunostained with CF660C, Magenta – WGA-CF680. Scale bar, 100 nm.

Supplementary Video 5: Raw camera images, organic dyes
Raw data from dSTORM imaging of Dy634, AF647, CF660C and CF680 at different excitation intensities, corresponding to Extended Data Figure 3. The movies are scaled from 0 – 900 photons per pixel and per frame. The photon counts reported in this manuscript correspond to merged localizations, i.e. are the photons summed over all pixels in the point-spread-function and summed over all consecutive frames in which a fluorophore is in its bright state.

Supplementary Video 6: High precision NPC
3D reconstruction of an individual nuclear pore complex from a low intensity, slow dSTORM acquisition of Nup96-SNAP BG-AF647 shown in Figure 2c, d.

Supplementary Video 7: Blinking buffer long-term stability
Time-lapse video of imaging chambers filled with glucose oxidase/catalase buffer, either unsealed (left) or sealed with parafilm (right). The buffer was supplemented with 0.005 % w/v phenol red which changes its color from red to yellow when the pH changes from pH 8 to pH 6. Corresponding to Extended Data Figure 8.

Supplementary Video 8: Raw camera images, photoconvertible protein
Raw data from PALM imaging of Nup96-mMaple corresponding to the reconstruction shown in Figure 2e.

Supplementary Dataset 1: Summary of all data
Spreadsheet containing data of individual analyzed cells.